CHAPTER 4

DEVELOPMENT AND EVALUATION OF CHOLECALCIFEROL LOADED LIPID-POLYMER HYBRID NANOPARTICLES

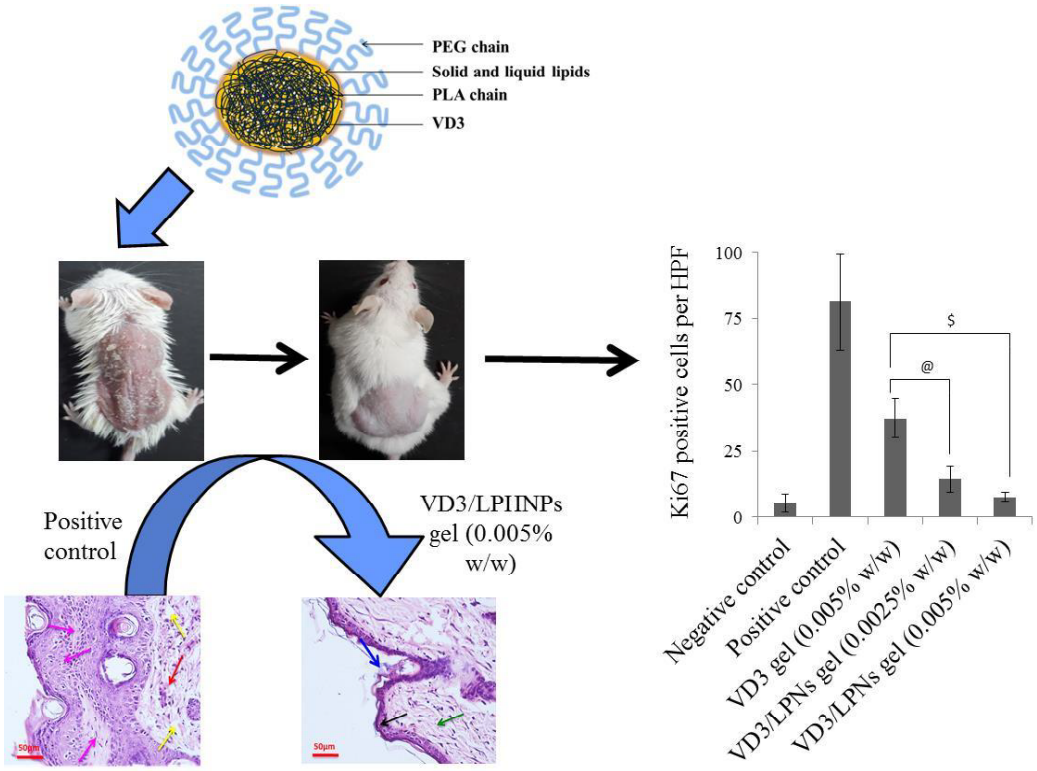

- **Introduction**
- **Experimental section**
- **Results**
- **Discussion**
- **Conclusion**

1. Introduction

Globally, 1–3% of the population is affected by psoriasis, a chronic inflammatory dermatological disease characterized by erythema, silvery-white scales, hyperkeratosis, abnormal differentiation and hyperplasia of epidermal keratinocytes [1-3]. The epidermal turnover rate in psoriasis is remarkably dropped to 1.5-3 days from the normal 30 days cycle. The accessible therapies for psoriasis can be broadly classified into systemic, phototherapy, and topical. The systemic therapy and phototherapy are restricted for the treatment of the severe type of psoriasis due to the associated toxicity issues [4,5]. Topical therapy approaches are comparatively much safer as the drugs are targeted to the desired site where the disease originates, eliminating unnecessary exposure to remaining body organs [6,7]. Several topical formulations are available for psoriasis patients that are composed of corticosteroids, anthralin, salicylic acid, coal tar, synthetic vitamin D3 and its analogues, and vitamin A. Amongst the above topical agents, molecules from vitamin D3 class finds significantly important place after corticosteroids as a monotherapy or combination therapy [8].

Cholecalciferol or vitamin D3 (VD3) is synthesized in the skin from a steroid hormone, 7-dehydrocholesterol, upon exposure to UVB radiation, or it can be obtained directly from dietary sources, which is further converted into more potent analogue calcitriol in the presence of enzymes (CYP27A1 and CYP27 B1) within keratinocytes [9-13]. Further, the cholecalciferol being the original form of VD3, does not exert hypercalcemic effect, erythema or burning sensation, which is reported to be with calcitriol and its other analogues [14,15]. It is very well established that VD3 and its analogues exhibit antipsoriatic properties by inhibiting proliferation (by decreasing the expression of cyclin D and c-myc and increase in expression of p21cip and

p27kip), promoting differentiation (increasing the expression of involucrin, transglutaminase, loricrin and filaggrin) and inducing apoptosis (secretion of ceramides) of keratinocytes, with its additional anti-inflammatory actions (by suppressing the secretion of IL-1α, IL-1β, IL-12/23 p40, TNF- IL-1α, inflammatory peptides (psoriasin and koebnerisin)). The mechanism behind these pharmacological effects is not completely understood, but these effects are produced at the genomic level mediated *via* VD3 receptor-retinoic X receptor heterodimeric complex formation that alters gene transcription (Vitamin D response elements (VDREs)) [11]. It has been previously reported that serum levels of calcitriol (10^{-11} to 10^{-10} M) are very low to induce VD3 receptor-mediated antipsoriatic effects in the skin. Several studies have reported that when the serum level of calcitriol exceeds 10^{-8} M, then it would be able to inhibit normal human keratinocytes *in vitro,* which is a highly unphysiological condition [11]. It was found that oral administration of vitamin D failed to improve the skin condition of psoriatic patients with the additional occurrence of significant toxicity due to its hypercalcemic effect [16]. This might be due to very high plasma protein binding (> 99%) of this molecule, and insignificant quantities of the drug are delivered to the desired site of action.

After the discovery of VD3 receptors on keratinocytes and fibroblasts, the drug delivery focus was directed from oral towards topical. Cholecalciferol or vitamin D3 (VD3) is highly lipophilic (log P-7.5) and susceptible to physical, chemical or biological degradation enforcing the challenges for topical delivery [17,18]. The epidermal keratinocyte proliferation process begins from the innermost layer of the epidermis, i.e., stratum basale that is placed just above the dermis and cells are transited from stratum basale towards the uppermost stratum corneum layer upon the progression of cell proliferation. The dermis is positioned just below the stratum basale and is provided with a rich source of blood capillaries, hair follicles, lymphatic vessels, sweat

glands and nerves. An ideal drug delivery system to treat psoriasis should penetrate into the deeper skin layers i.e., viable epidermis and dermis, without entering the systemic compartment and show a prolonged drug release profile [19,20].

Nanoparticle based topical drug delivery strategies (including both lipidic and polymeric) have provided promising options over conventional drug delivery (ointments, creams and gels) by facilitating deep skin penetration and imparting slow and sustained drug release profile overcoming sudden high loco-regional exposure [19,21-26]. Tannaz et al. reported cholecalciferol loaded polymeric nanospheres (TyroSpheres) delivered significantly high quantities of the drug in epidermis compared to the free drug [18]. Amanpreet et al. reported an improved *in vivo* antipsoriatic activity of clobetasol propionate and calcipotriol (a vitamin D analogue) when delivered as a nanoemulsion-based gel compared to free drug and conventional marketed formulation [27]. Another reported evidence was provided from the research outcome of Rahul et al., claiming that there was improved *in vivo* antipsoriatic efficacy after delivering gel containing betamethasone dipropionate and calcipotriol loaded solid lipid nanoparticles compared to their commercially available conventional product i.e., Daivobet ointment [28]. Rhythm et al. demonstrated a significant enhancement in antipsoriatic efficacy after delivering cyclosporine and calcipotriol in the form of nanostructured lipid carriers compared to the conventional marketed product [29].

Both lipidic (microemulsions, nanostructure lipid carriers (NLC), solid lipid nanoparticles (SLN), niosomes, liposomes, self-emulsifying drug delivery systems (SEDDS) and micelles) and polymeric (polymeric micelles, polymer-drug conjugate and polymeric nanoparticles) nano-carriers have their associated advantages and disadvantages. In order to get

benefits of both lipidic and polymeric nano-carriers along with avoiding their disadvantages, a newer class of nano-carriers has been developed that demonstrated improved drug loading capacities, higher cellular uptake, a more controlled drug release profile and biocompatibility as reported elsewhere [30]. In chapter 3, we reported the nano-formulation based platform technology consisting of multi-component clobetasol propionate (CP)-loaded monolithic lipid-polymer hybrid nanoparticles that demonstrated significant improvement in cellular uptake, penetration in deeper skin layers with imperceptible systemic leaching and proven enhanced *in vivo* antipsoriatic efficacy of clobetasol propionate [19]. To meet the safety profile of VD3 with simultaneous improvement in the *in vivo* antipsoriatic efficacy, a new formulation is required that will retain the drug in the deeper skin layers, control its release profile and reduces its systemic absorption. Current chapter demonstrates the applicability of LPNs in delivering the VD3 for improved antipsoriatic activity in swiss albino mice. Herein, we have formulated VD3 into the LPNs comprising of both solid and liquid lipids, along with amphiphilic di-block copolymer, followed by their thorough in vitro characterization. Further, *in vivo* assessment for efficacy has been performed in IMQ-induced psoriatic mice model using *Swiss albino* mice by assessing the PASI score and thorough histopathological and immunohistochemical examination after treatment with the developed formulations.

2. Experimental section

2.1.Materials

Cholecalciferol was obtained as a generous gift sample from Orbicular Pharmaceutical Technology Pvt. Ltd. (Hyderabad, India). Methoxy poly(ethylene glycol) (mPEG (Mn 5000 Da)), DL-lactide (DL-LA), and stannous octanoate ($Sn(Oct)_2$) were purchased from Sigma Aldrich (St. Louis, MO). Precirol® ATO 5 and Labrasol® were received as gift samples from

Gattefosse, (Lyon, France). Linoleic acid was procured from Acme Synthetic Chemicals (Mumbai, India). Carbopol 974P was obtained from Lubrizol, (OH, USA). Tween 80 was provided as a gift sample from BASF India Ltd, (Mumbai, India). IMQ was purchased as Imiquad®, a topical cream (5% w/w) from Glenmark, (Mumbai, India). Phosphate Buffered Saline (PBS) pH 7.4 was purchased from HiMedia Laboratories (Mumbai, India). HPLC grade methanol (MeOH), acetonitrile (ACN) and chloroform ($CHCl_3$) were procured from Merck Ltd., (Mumbai, India).

2.2. Synthesis and characterization of amphiphilic copolymer

Ring-opening polymerization (ROP) strategy was adopted for the synthesis of di-block copolymer (mPEG-PLA) by reacting DL-LA with chain initiator (mPEG) using catalyst ($Sn(Oct)_2$) as reported earlier [19]. Briefly, mPEG (0.216 g, Mn 5000 Da) was transferred to 10 mL microwave vial, and melted at 110 °C for 5 min followed by addition of DL-LA (0.636 g) and ($Sn(Oct)_2$) (10 mol % of mPEG dissolved in dried toluene) and subjected to further heating in monowave chamber (Monowave 400, Anton Parr, VA, USA) at 110 °C for 30 min to complete the reaction. Later obtained crude product was dissolved in $CHCl_3$, and subjected to further purification by precipitation using chilled diethyl ether, followed by drying and characterization by ^{1}H-NMR (AVANCE II Bruker 400 MHz spectrometer) and gel permeation chromatography (Waters 515 HPLC) as reported in chapter 3.

2.3. Formulation and development

2.3.1. Preparation and characterization of VD3/LPNs

Nanoparticle preparation method was adopted from chapter 3 with slight modification. Briefly, VD3 (7 mg), Precirol® ATO 5 (90 mg), mPEG-PLA (90 mg; molecular weight: 12927 Da) and linoleic acid (90 mg) were transfered to 25 mL round-bottomed flask (RBF) and the contents were dissolved using 800 μL of chloroform by warming at 40 ºC. The organic solvent was then removed by rotary evaporator (Buchi Rotavapor® R-300, Switzerland) at 60 °C for 30 min under vacuum to form a uniform film of a hybrid matrix. Aqueous tween 80 solution (1.5% w/v) was heated at 60 °C and added to the RBF containing the hybrid matrix maintained at 60 °C to form a dispersion that was subsequently transferred to a 15 ml glass vial and sonicated at 20% amplitude for 2 min at 60 °C using probe sonicator. The obtained hot colloidal dispersion was immediately cooled on an ice-water bath and centrifuged for 5 min at 5000 rpm to seperate the larger particles and unentrapped drug.

For the particle size and size distribution measurements, samples were prepared by diluting 200 µL of formulation in 2 mL of purified water followed by analysis for particle size and PDI using Malvern Zetasizer (Malvern Nano ZS). For zeta potential measurement, the LPNs were analyzed in undiluted form using Malvern Zetasizer. Morphology of VD3/LPNs was examined by FE-SEM (FEI Quanta FEG 250 SEM, Hillsboro, Oregon, Washington). The encapsulation efficiency was estimated by RP-HPLC based analytical method as reported in chapter 2.

2.3.2. In vitro drug release study and release kinetics

In order to have an estimate of VD3 release from these LPNs, in vitro release study was carried out using a destructive sampling technique wherein the VD3/LPNs were dispersed in release media (900 µL PBS buffer pH 7.45 containing 5% w/v Labrasol) in 2 mL eppendorf tubes and kept in an orbital shaker at 37ºC. At specified time points (i.e. 0.25 h, 0.5 h, 1 h, 2 h, 4 h, 8 h, 12 h, 1 day, 2 day, and 3 day), contents from eppendorf tubes were subjected to ultracentrifugation (Sorvall™ MX Plus Series, Thermo Scientific™, Mumbai, India) at 1,40,000 rpm for 1h 10 min at 25°C and the supernatant was subjected to RP-HPLC analysis using the developed analytical method to determine the quantity of VD3 released and cumulative percent (%) drug release was plotted against time (h). The release kinetics was predicted using DDSolver software add-in program by fitting the release profile into different kinetic models.

2.3.3. Preparation and characterization of topical gel containing VD3/LPNs (VD3/LPNs gel)

VD3/LPNs gel (VD3 ≈ 0.005% w/w; 100 g) was formulated using carbopol 974P as a gelling agent at 0.75% w/w. For this, 0.75 g of carbopol 974P was hydrated overnight in a beaker with purified water (10 ml). VD3/LPNs (VD3 ≈ 0.005% w/w) was added to the hydrated carbopol 974P and mixed uniformly using a glass rod. Propylparaben (0.3 g), methylparaben (0.3 g) and propylene glycol (13 g), were homogeneously mixed with the above-hydrated mixture. Its weight was adjusted to 95 g by using purified water followed by pH adjustment to 6.8 by using 1 M NaOH to obtain a gel. Further, final weight was adjusted to 100 g using purified water and stirred homogenously to obtain a visually uniform gel. Blank LPNs, VD3/LPNs and their corresponding gels were freeze dried (FreeZone Triad® Benchtop Freeze Dryers (Labconco,

MO, USA)) followed by their characterization using FTIR (Bruker Apha, MA, USA) and DSC (DSC-60 Plus Shimadzu, Kyoto, Japan). Further, the rheological studies of the VD3/LPNs gel (250 mg) were carried out using a Rheometer (MCR 92, Anton Paar, Germany) to determine its viscosity (mPa.s) and graphs of shear stress versus shear rate and viscosity versus shear rate were generated as reported previously [19]. Additionally, the influence of temperature on the viscosity of the final product was investigated. Further, oscillatory rheological studies, including amplitude sweep test and frequency sweep test were performed at 25 °C with 0.2 mm gap. Initially, an amplitude sweep test was conducted on the sample to define the linear viscoelastic (LVE) region at a fixed frequency of 10 rad/s, a strain (γ) varying from 1 to 100%. Subsequently, the frequency sweep test of gel was carried out in the frequency range 0.1–100 rad/s by subjecting to deformation within the LVE region and the physical stability of the gel was predicted.

2.4. In vivo efficacy studies

2.4.1. Design of study protocol and establishment of in vivo psoriatic mice model

IMQ exerts potent immune-stimulatory action mediated *via* TLR7/8 receptors and can be used topically to induce psoriasis-like dermatological reaction resembling clinical conditions for in vivo antipsoriatic testing [31-33]. The study protocol was duly approved by the Institutional Animal Ethics Committee (IAEC) (protocol no: IAEC/RES/25/11), and the experiment was performed as per CPCSEA guidelines. One week prior to the initiation of the experiment, animals were acclimatized in well-ventilated plastic cages under standard laboratory conditions with 12 h light and 12 h dark cycle. Experimental protocol for the development of the IMQ-induced psoriasis-like mouse model is demonstrated in Figure 5. Swiss albino mice (female, 10

to 12 weeks old) were randomly divided into five groups (n=6) i.e. group 1 (Negative control (kept without any treatment: IMQ or test product)), group 2 (Positive control (treated with only IMQ but no test product)), group 3 (free VD3 gel (0.005% w/w)), group 4 (VD3/LPNs gel (0.0025% w/w)) and group 5 (VD3/LPNs gel (0.005% w/w)). All the three test groups mentioned above (group 3, 4 and 5) received 40 mg/cm^2 of respective gels. Mice from Group 2 to 5, were treated topically on their shaved back skin (BS) and right ear (ES) with 62.5 mg of Imiquad® (5% w/w) for 5 consecutive days, translating a daily dose of 3.125 mg of the imiquimod (IMQ) whereas, Group 1 (Negative control) mice were not subjected to IMQ treatment and these resembles healthy animals.

2.4.2. Evaluation parameters

The *in vivo* antipsoriatic efficacy was determined by a scoring system that was developed based on the clinical Psoriasis Area and Severity Index (PASI). Scoring for the erythema, scaling and thickening were done independently on a scale range 0 to 4 (where numbers indicate the extent of the specified parameter i.e. 0 (none), 1 (slight), 2 (moderate), 3 (marked), 4 (very marked)). Cumulative scoring (sum of erythema plus scaling plus thickening) that indicated the degree of inflammation was measured on a scale from 0 to 12.

Measurement of back skin thickness and ear thickness (both left and right, where left ear served as a control) were done using vernier caliper and digital micrometer respectively on a daily basis. An increase in the both right ear thickness compared to the left ear and back skin thickness was due to induced inflammatory response indicating the degree of psoriasis. Variation (% change) in body weights of animals during the entire study duration was determined. At the end of the study i.e., day 5, animals were sacrificed and various tissues such as right ear, back skin, spleen and liver were isolated. Spleens from all the groups were compared for size and their

average weights. Isolated tissues were subjected to histopathological examination by Hematoxylin and Eosin (H&E) staining for determining the extent of damage that has occurred. For skin samples (both back skin and right ear), total skin damage score was determined that included cumulative scoring consisting of the sum of damages due to various psoriatic parameters like parakeratosis, hyperkeratosis, epidermal hyperplasia, angiogenesis, suprapapillary thinning, inflammatory infiltrates, pustule of Kogoj, munro's microabscess. For liver samples, total liver damage score was determined from the summation of parameters such as degeneration of hepatocytes and infiltration of inflammatory cells. For spleen samples, total spleen damage was studied that include parameters such as integrity of splenocytes and depopulation of lymphocytes. Further, Ki67, a cell proliferation marker expressed in animals back skin was examined immunohistochemically (IHC) and the result was reported as the average number of Ki67 positive cells stained per high power field that was directly correlated to the degree of psoriasis induced.

2.5. Statistical analysis

Analyses were carried out using GraphPad Prism (GraphPad Software (version 8), La Jolla, CA, USA). All the quantitative data are presented as mean ± standard deviation (SD) or standard error of the mean (SEM) and significant differences between two or more treatment groups were determined with analysis of variance (ANOVA) followed by Tukey's test wherein p-value ≤ 0.05 was considered statistically significant.

3. Results

3.1. Characterization of VD3/LPNs and VD3/LPNs gel

Hot homogenization method produced nanoparticles of smaller size 123.1 ± 6.16 nm, narrow PDI 0.234 ± 0.03, zeta potential -4.33 ± 0.85 mV, and percent encapsulation efficiency 76.80 ± 1.36%. Nanoparticle dispersion showed on bench stability for one day without any significant change in particle size and polydispersity index evident from the particle size and size distribution data Figure 4.1. The FE-SEM image demonstrated that VD3/LPNs exhibited

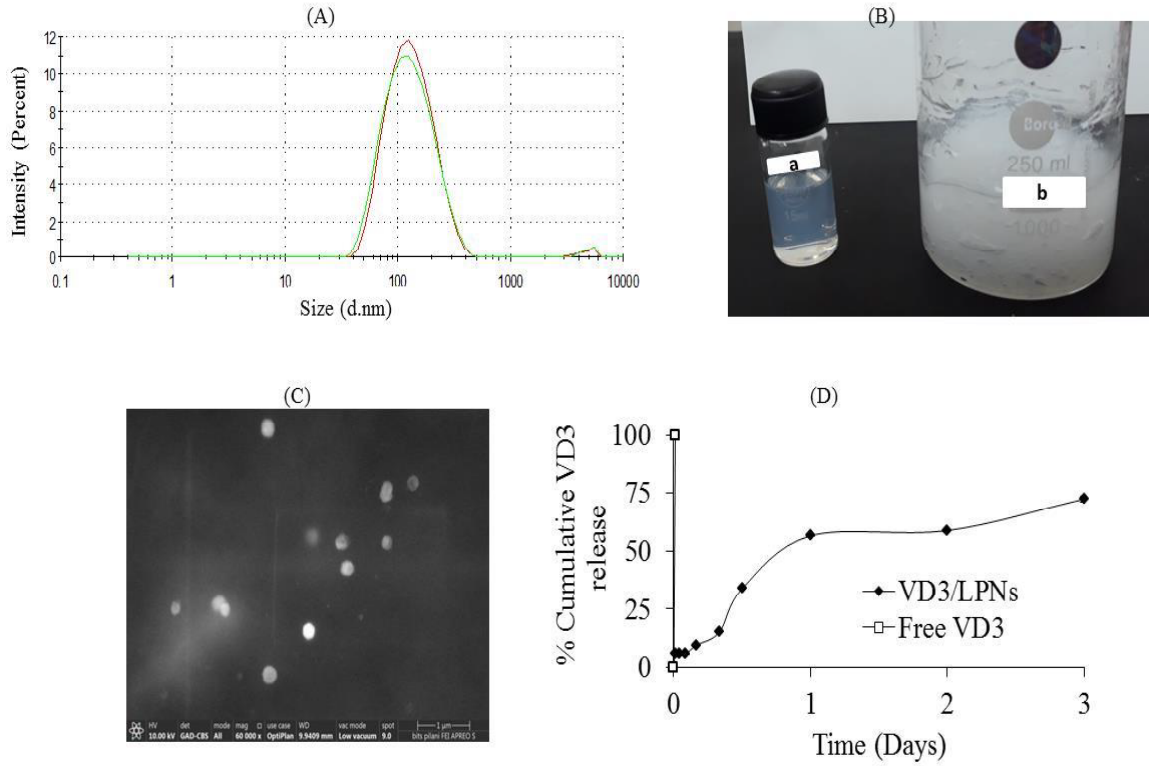

Figure 4.1. Characterization of VD3/LPNs. (A) Dynamic light scattering (DLS) measurements of size distribution of freshly prepared VD3/LPNs (red plot) and VD3/LPNs stored at room temperature for one day (green plot) in water determined by Malvern zetasizer, (B) photographic images of (a) VD3/LPNs dispersion and (b) VD3/LPNs gel (0.005% w/w), (C) field emission-scanning electron microscopic images of VD3/LPNs (scale bar = 1 μm), and (D) In vitro drug release from VD3/LPNs showing a sustained release profile compared to it free form i.e. free VD3. Error bars indicate mean ± SD.

spherical morphology with no visible aggregation. *In vitro* drug release studies indicated that VD3/LPNs showed sustained drug release of 72.48 ± 1.27% at the end of 3 days with no burst release whereas, free VD3 was released completely within 15 min, indicating that sink condition was maintained. Release data were fitted into various models including Higuchi, Zero-order, Hixson-Crowell, Korsemeyer-Peppas and First-order and it was found that drug release pursued Korsemeyer-Peppas model (R^2 = 0.9339) with n-values of 0.545, signifying that the release

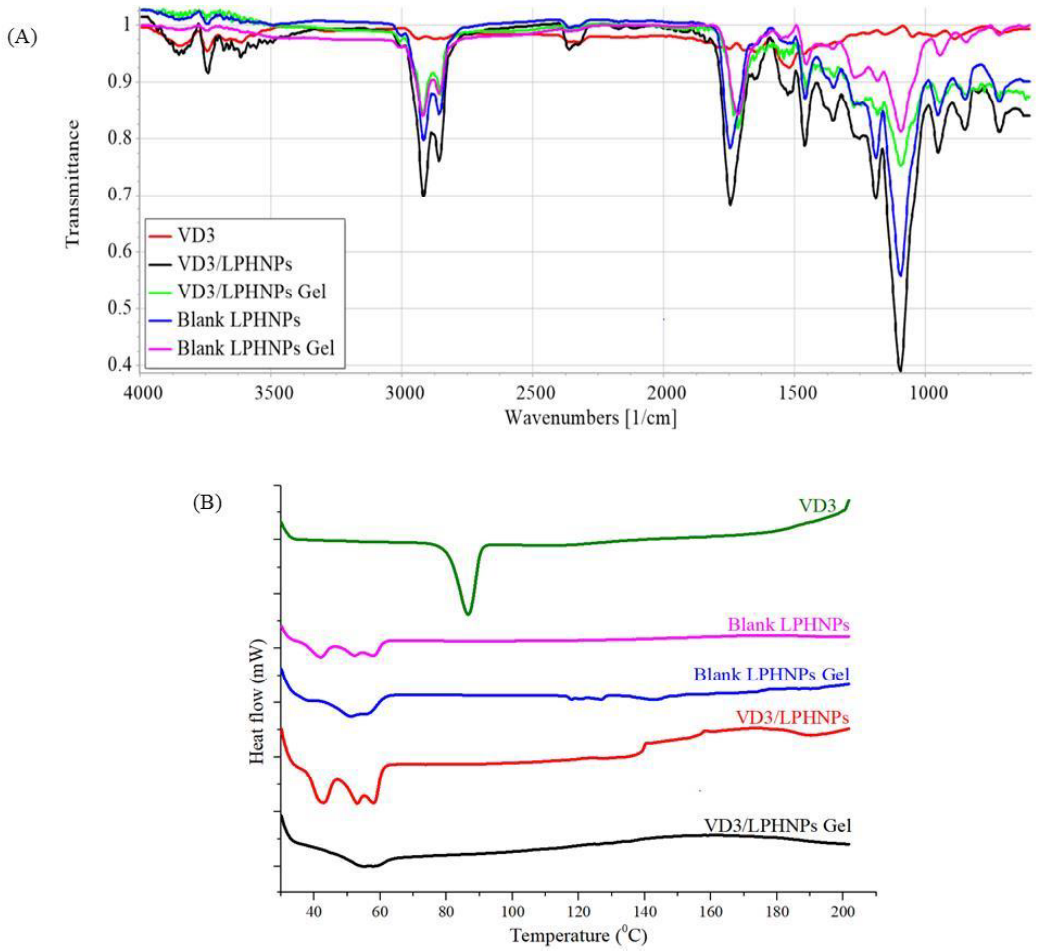

Figure 4.2. (A) FTIR spectra of pure VD3, VD3/LPNs, VD3/LPNs gel, blank LPNs and blank LPNs gel and (B) DSC thermograms of pure VD3, blank LPNs, blank LPNs gel, VD3/LPNs and VD3/LPNs gel.

mechanism involved non-fickian diffusion or anomalous diffusion.

As depicted in Figure 4.2(A), the FTIR spectrum of VD3 showed its representative peaks at 3281 cm^{-1} (O-H stretch), 2939 cm^{-1} (CH_3 asymmetric stretching), 2872 cm^{-1} (CH_2 symmetric stretching), 1518 cm^{-1} (C=C stretch). FTIR spectrum of VD3/LPNs and VD3/LPNs gel revealed absence of most of these characteristic drug peaks which could be probably due to the loading of active into the nanoparticles core and lower drug/feed material ratio. Furthermore, the FTIR spectrum of VD3/LPNs gel and VD3/LPNs did not differ significantly from blank LPNs gel and blank LPNs, respectively. It was evident from the FTIR spectra that in case of blank LPNs gel and VD3/LPNs gel, there was slight reduction in the intensity of peaks in comparision to the blank LPNs and VD3/LPNs respectively signifying interaction between the nanoparticles and gelling agent (carbopol). A sharp endothermic peak corresponding to melting point of VD3 was detected at 86 °C in the DSC thermogram of VD3 indicating its crystallinity Figure 4.2(B). However, the DSC thermogram of VD3/LPNs and VD3/LPNs gel revealed absence of melting point of drug indicating its transformation to amorphous form after loading into the nanoparticles.

Viscocity (η) of VD3/LPNs gel was found to be 10836 mPa.s at constant shear rate of 10 s^{-1} and 25 °C possessing ideally desirable non-newtonian flow properties with characteristic shear-thinning behaviour and variable thixotropy revealed from shear stress (mPa) versus shear rate (1/s) and viscosity (η) versus shear rate (1/s) graphs Figure 4.3. Value of LVE region of the gel obtained from amplitude sweep test was found to be 2.24% wherein the storage modulus (G') was found to be greater than loss modulus (G") i.e. G' > G" suggesting formation of gel structure possessing viscoelastic character. Further, the long term stability of gel was demonstrated from

the frequency sweep test graph, where G' > G" in lower frequency range thus fulfilling the precondition for long term storage stability.

3.2. In vivo efficacy studies

3.2.1. Psoriasis Area Severity Index (PASI) evaluation

The in vivo antipsoriatic efficacy of VD3/LPNs gel was evaluated using IMQ-induced psoriatic mice model in *Swiss albino* mice based on clinical Psoriasis Area Severity Index (PASI) system. Figure 4.4 showed that in positive control group, cumulative score (sum of

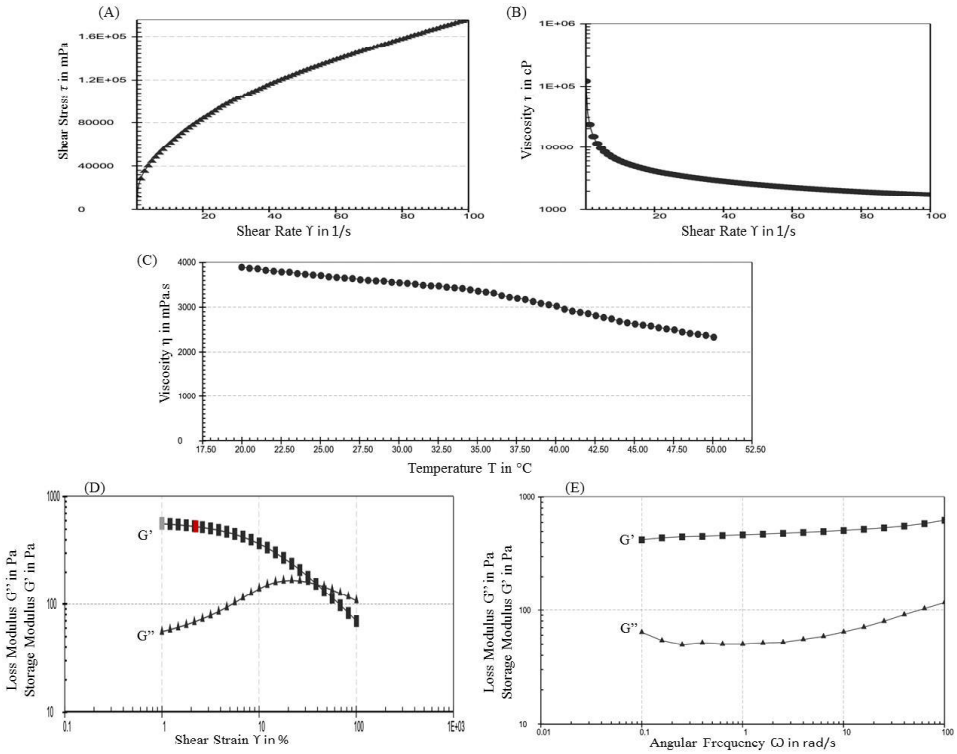

Figure 4.3. Rheological and oscillatory rheological measurements of VD3/LPNs gel suggested non-newtonian flow properties possessing shear-thinning behaviour with variable thixotropy as apparent from (A) shear stress (mPa) versus shear rate (1/s) and (B) viscosity (η) versus shear rate (1/s) graphs, (C) subjecting to rise in temperature did not showed sudden collapse of gel 3D matrix structure evident from viscosity (mPa.s) versus temperature (°C) graph suggesting stability of matrix, (D) formation of viscoelastic gel with G' (storage modulus) > G" (loss modulus) within the LVE region in amplitude sweep test, and (E) long term storage stability was predicted from frequency sweep test where G' > G" in lower frequency range.

erythema plus scaling plus thickening) began to increase significantly from day 1 and got roused up to day 5 with cumulative score of 9.00. It can be observed that all the three groups treated with VD3 formulations i.e. conventional product (VD3 gel (0.005% w/w)) and test products (VD3/LPNs gel at both strengths i.e. (0.0025% w/w and 0.005% w/w)) were able to reduce the psoriatic parameters drastically with cumulative score of 4.40, 2.60 and 0.00 respectively on day

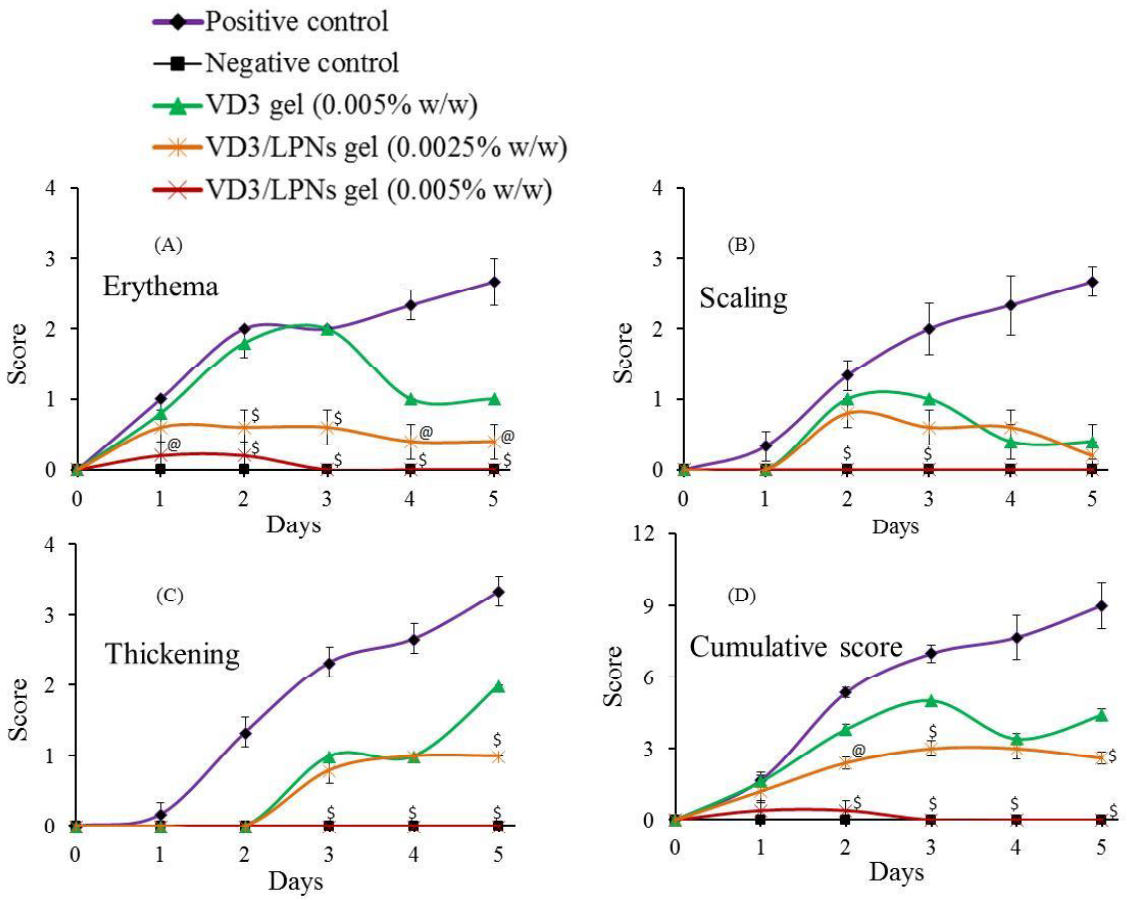

Figure 4.4: VD3/LPNs gel suppressed IMQ-induced inflammatory psoriatic condition in mice. Scores of various psoriatic parameters based on PASI system measured on scale from 0-4 on the days indicated that includes (A) erythema, (B) scaling, and (C) thickening, Additionally (D) cumulative score representing the degree of psoriasis that includes sum of erythema, scaling and thickening measured on scale from 0-12 on the days indicated. Each value is denoted as mean ± SEM. @, $p \leq 0.05$ and $, $p \leq 0.01$, versus VD3 gel (0.005% w/w) treated group.

5 indicating significant improvement in efficacy of VD3 when delivered as lipid-polymer hybrid nanoparticles.

3.2.2. Measurement of right ear (ES) and back skin (BS) thickness

There was significant increase of both ES and BS thickness of mice on application of imiquimod, which acts via TLR7/8 receptors to exert potent immune stimulatory action resulting into dermal inflammation followed by hyperplasia of keratinocytes. Reduction of the thickness and bringing it back to normal indicated effective treatment of psoriasis. Figure 4.5, demonstrated that in positive control animals, the ES thickness got gradually augmented from 0.263 mm (day 0) to 0.340 mm (day 5) whereas the BS thickness was progressively augmented from 1.338 mm (day 0) to 2.318 mm (day 5). In case of VD3/LPNs gel (0.0025% w/w) treated animals, ES thickness was increased from 0.270 mm (day 0) to 0.296 mm (day 5) and BS thickness was increased from 1.340 mm (day 0) to 1.588 mm (day 5) that was comparable to that of conventional product i.e. VD3 gel (0.005% w/w) which showed increase in the right ear thickness from 0.268 mm (day 0) to 0.300 mm (day 5) and BS thickness was increased from 1.274 mm (day 0) to 1.588 mm (day 5). VD3/LPNs gel (0.005% w/w) treated group demonstrated least change in the ES and BS thickness and was equivalent to negative control group suggesting most effective treatment.

3.2.3. Measurement of average spleen weights

Imiquimod treatment results into inflammation of spleen leading to significant higher weights and sizes of spleens in case of positive control group (298.57 mg) compared to negative control group (58.97 mg) Figure 4.6(A). Reduction of the average weight of spleen indicated effective treatment of psoriasis. The group treated with VD3/LPNs gel (0.0025% w/w) showed relatively lower average spleen weights (113.66 mg) compared to group treated with VD3 gel

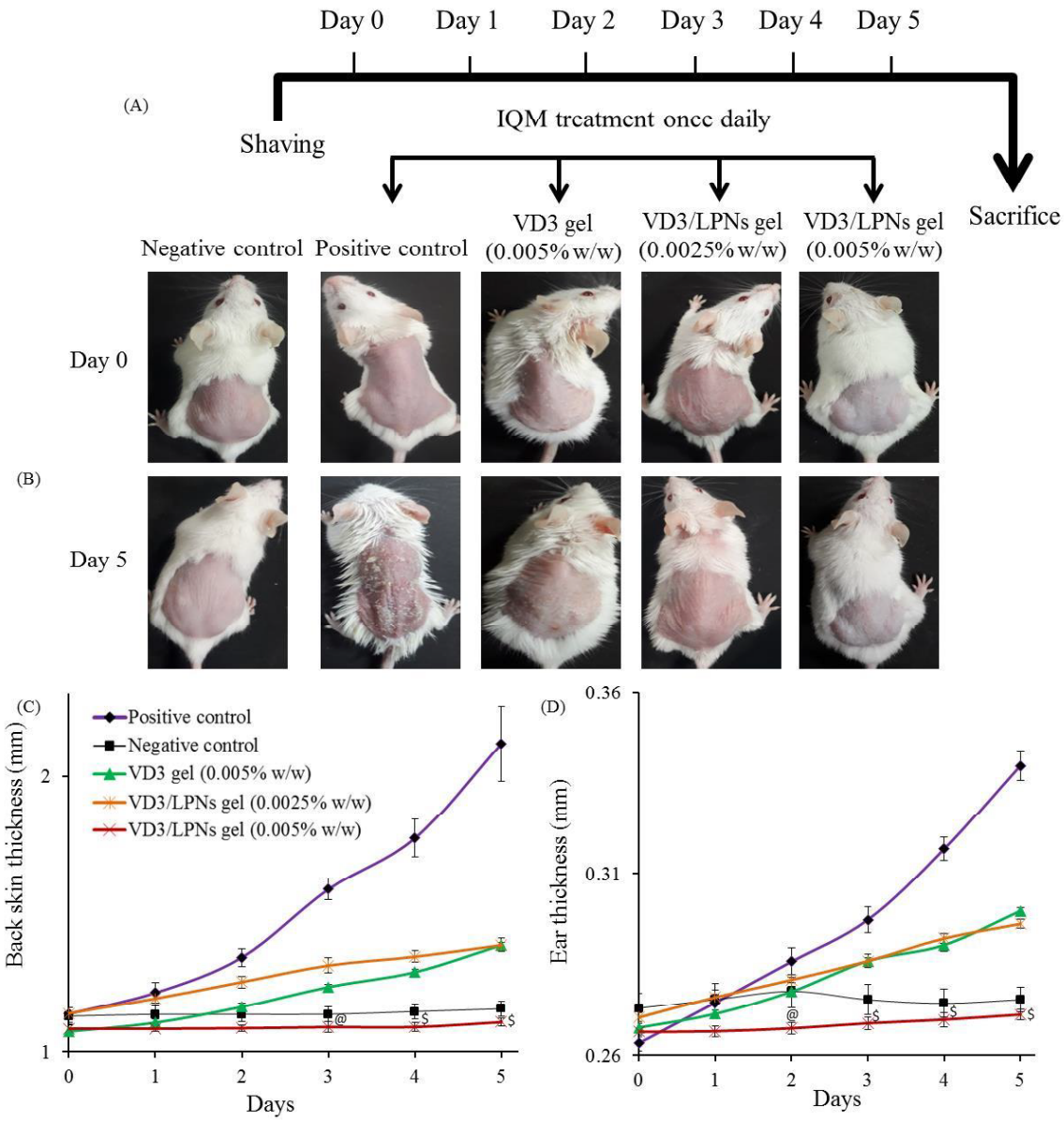

Figure 4.5. IMQ-induced psoriatic mouse model resembles the clinical psoriasis condition. Swiss albino mice were subjected to topical treatment on daily basis with IMQ on the right ear and back skin. (A) In vivo study protocol for IMQ-induced psoriatic mice model, (B) photographic images of back skin of mouse from various groups on day 0 and day 5, measurement of (C) back skin (BS) and (D) right ear (ES) thickness using digital vernier caliper and micrometer respectively. Each value is denoted as mean ± SEM. @, $p \leq 0.05$ and $, $p \leq 0.01$, versus VD3 gel (0.005% w/w) treated group.

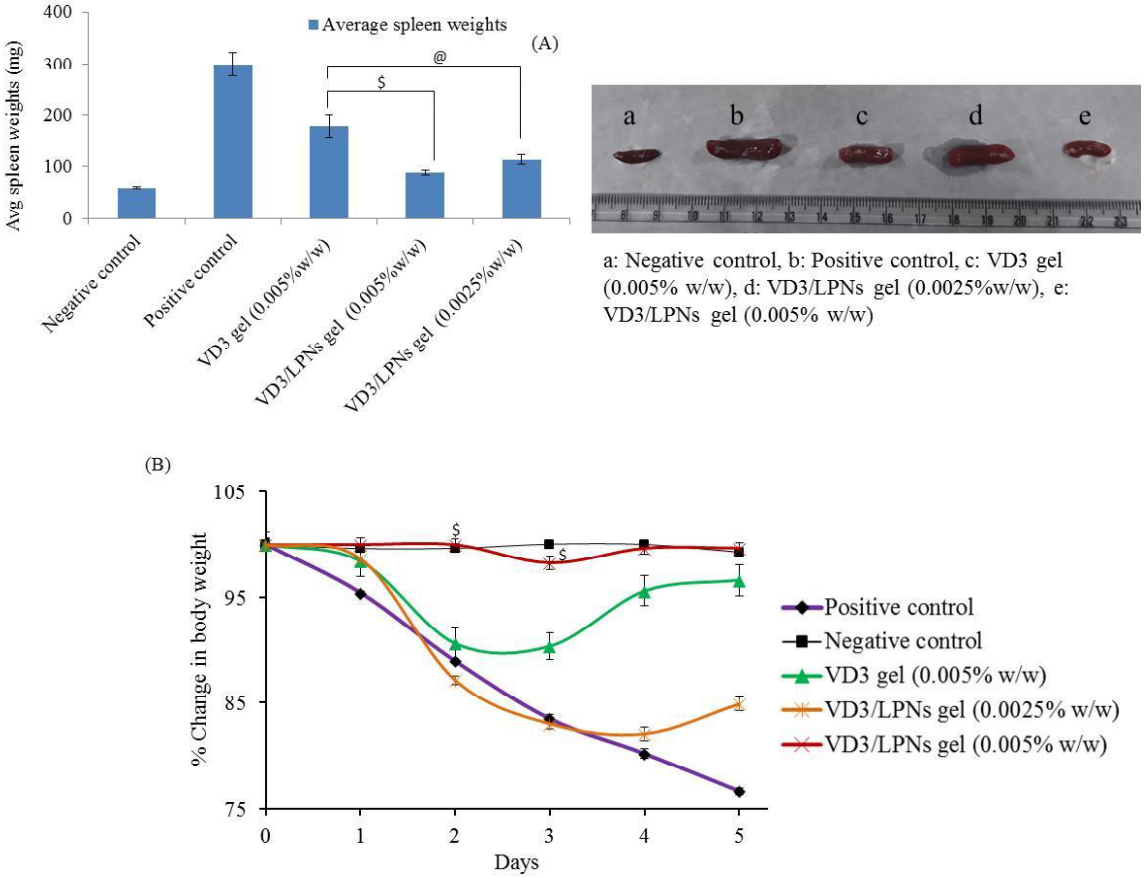

Figure 4.6. Topical treatment with IMQ results into enlargement of spleen shown in positive control group. VD3/LPNs gel showed significant reduction in the spleen weights. (A) Average spleen weights from various groups, along with their comparative spleen size s viz. (a) negative control, (b) positive control, (c) VD3 gel (0.005% w/w), (d) VD3/LPNs gel (0.0025% w/w), (e) VD3/LPNs gel (0.005% w/w). During the study duration, application of IMQ leads to substantial toxicity resulting into fluctuation in body weights with significant reduction in the values from their original ones. (B) percent change in body weight indicating complete recovery in groups treated with VD3/LPNs gel. Each value is denoted as mean ± SEM. @, $p \leq 0.05$ and $, $p \leq 0.01$, versus VD3 gel (0.005% w/w) treated group.

(0.005% w/w) that showed average spleen weights (178.69 mg) indicating enhancement in the in vivo efficacy. The group treated with VD3/LPNs gel (0.005% w/w) showed least value of average spleen weight (88.35 mg) that was equivalent to that of negative control group.

3.2.4. Measurement of percent change in body weights

During the entire study, animals from negative control group did not displayed any significant fluctuation in body weights. In positive control, there was significant fluctuation in body weights of animals during the study duration and their weight was reduced by 23% (day 5). Group treated with VD3/LPNs gel (0.005% w/w) showed least fluctuation in body weights and there was no significant reduction in body weights (day 5) which was comparable to negative control group suggesting effective treatment Figure 4.6(B).

3.2.5. Histopathology and immunohistochemistry (IHC)

Figure 4.7(A), shows the Hematoxylin and Eosin stained histopathological sections of the right ear (ES) skin and back skin (BS). For comparing the efficacy of various treatments, total damage score of all the three organs i.e. skin (ES and BS), liver and spleen were compared. The presence of munro's microabscess (sky blue arrow) and Pustule of Kogoj (pink arrow) in ES and BS of positive control animals indicated potent induction of psoriasis. It was observed that in all the three groups treated with VD3 containing formulations, these potential parameters were absent indicating the effectiveness of VD3 in treating psoriasis. Total skin damage score was calculated from the summation of various psoriatic parameters that included parakeratosis, hyperkeratosis, angiogenesis, hyperplasia, inflammatory infiltrates, suprapapillary thinning, pustule of Kogoj and munro's microabscess. It can be observed from the that right ear of group treated with conventional product i.e. VD3 gel (0.005% w/w) showed the presence of rete ridges (shown in red circular mark) which is a characteristic of psoriasis indicating that treatment was not that effective compared to the VD3/LPNs gel where this psoriatic parameter was absent. It was observed that the total skin damage score (both right ear and back skin) for group treated

with VD3/LPNs gels were found to be significantly lower compared to group treated with conventional product Figure 4.7(B).

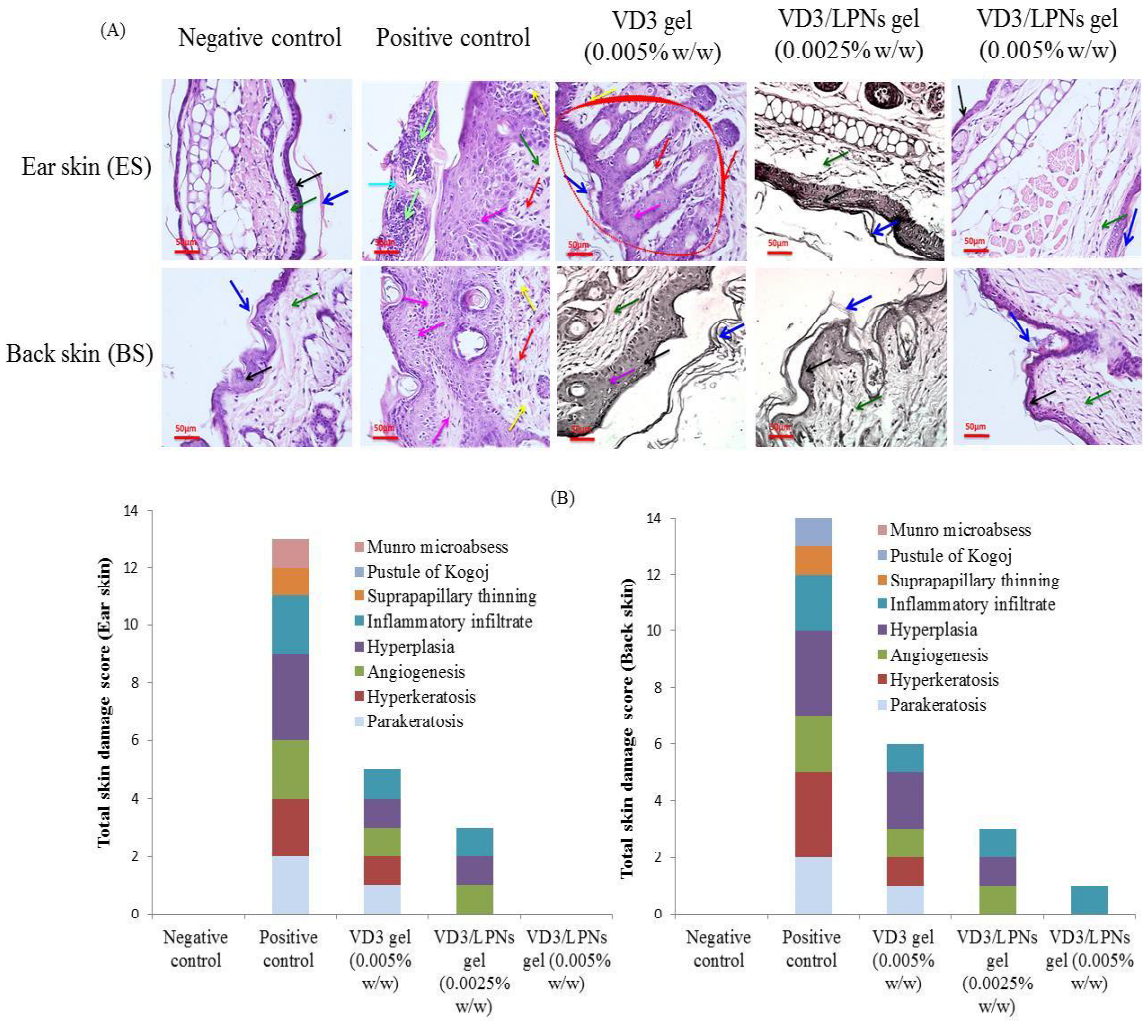

Figure 4.7. (A) Histopathological examination (H&E, Magnification: 40X) of right ear skin (ES) and back skin (BS) of animals from various groups. For **ES** and **BS,** arrow acronyms are as follow- **Black:** Epidermis; **Pink:** Pustule of Kogoj; **Dark green:** Dermis; **Sky blue:** Munro microabscess; **Red:** Infiltration of inflammatory Cells; **Blue:** Stratum Corneum; **Yellow:** Capillary Proliferation; **White:** Parakeratosis; **Purple:** Epidermal Hyperplasia; **Fluorescent green:** Hyperkeratosis. Scale bar = 50 µm and (B) Assessment of various psoriatic parameters representing total skin damage score for both right ear and back skin of various groups.

The association of liver fibrosis with cutaneous inflammation in IMQ-induced mice model was previously reported [34]. Figure 4.8(A), shows the Hematoxylin and Eosin stained

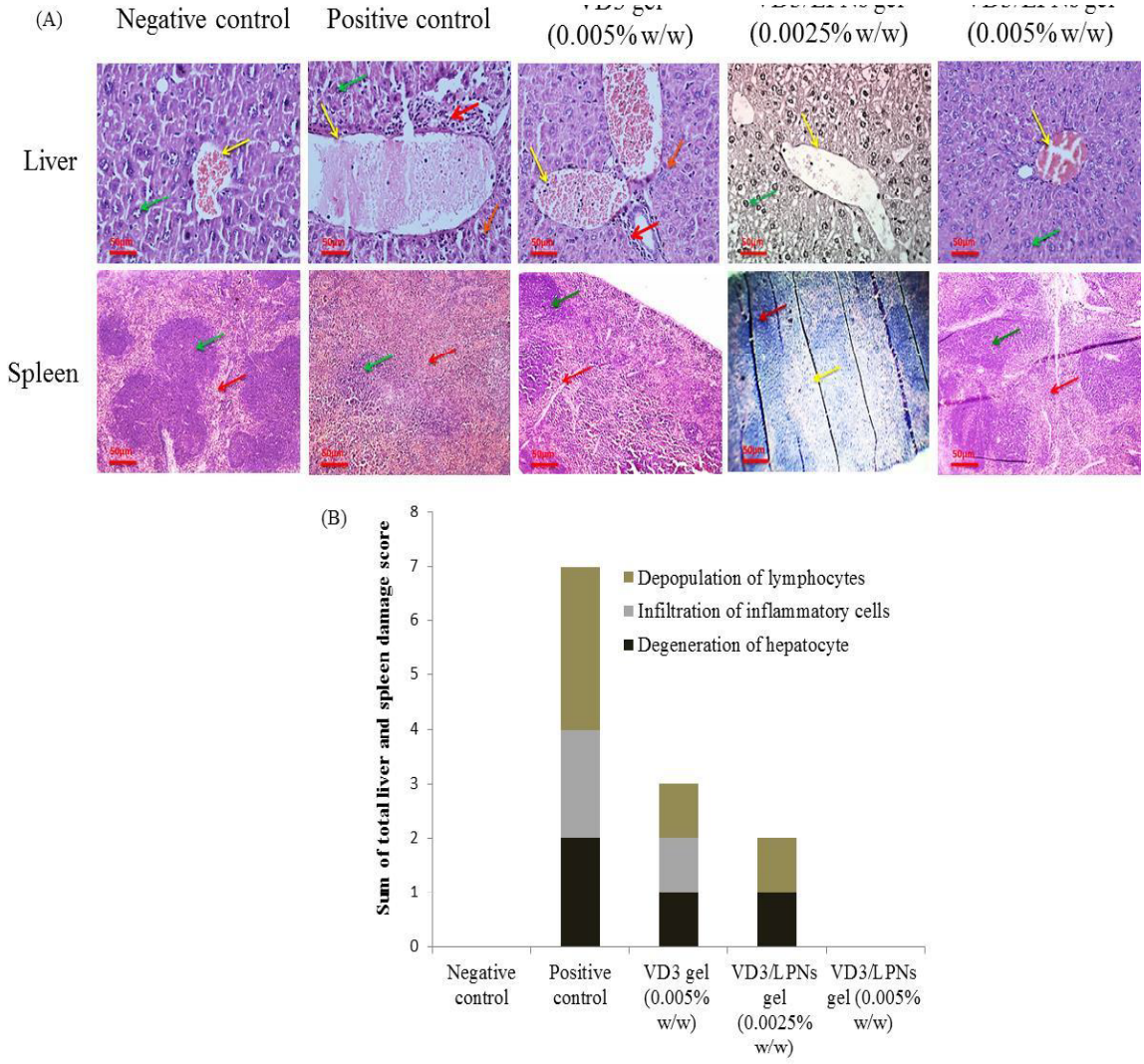

Figure 4.8. (A) Histopathological examination (H&E) of liver and spleen of animals from various groups. For **liver (**Magnification: 40X**),** arrow acronyms are as follow- **Red:** Infiltration of mononuclear inflammatory Cells; **Green:** Hepatocytes; **Yellow:** Central vein; **Orange:** Hepatocytes degeneration. For **spleen (**Magnification: 10X**),** arrow acronyms are as follow- **Green:** White pulp; **Red:** Red pulp. Scale bar = 50 µm and (B) Assessment of various psoriatic parameters representing sum of total liver and spleen damage scores of various groups.

histopathological sections of the liver and spleen. It was observed from the histopathological data that IMQ treatment results into hepatic damage due to infiltration of inflammatory cells from central vein along with hepatocyte degeneration in positive control. Inhibition of these two parameter leads to lowering of total liver damage score marking the efficacy of treatment. Histopathological samples of spleen demonstrated that in positive control group on application of imiqimod, resulted into undistinguished areas of red pulp (pink in colour) and white pulp (blue in colour) which was due to rupture of spleenocytes upon swelling and enlarging of spleen. The effectiveness of treatment was based on regaining of distinguished areas of red pulp and white

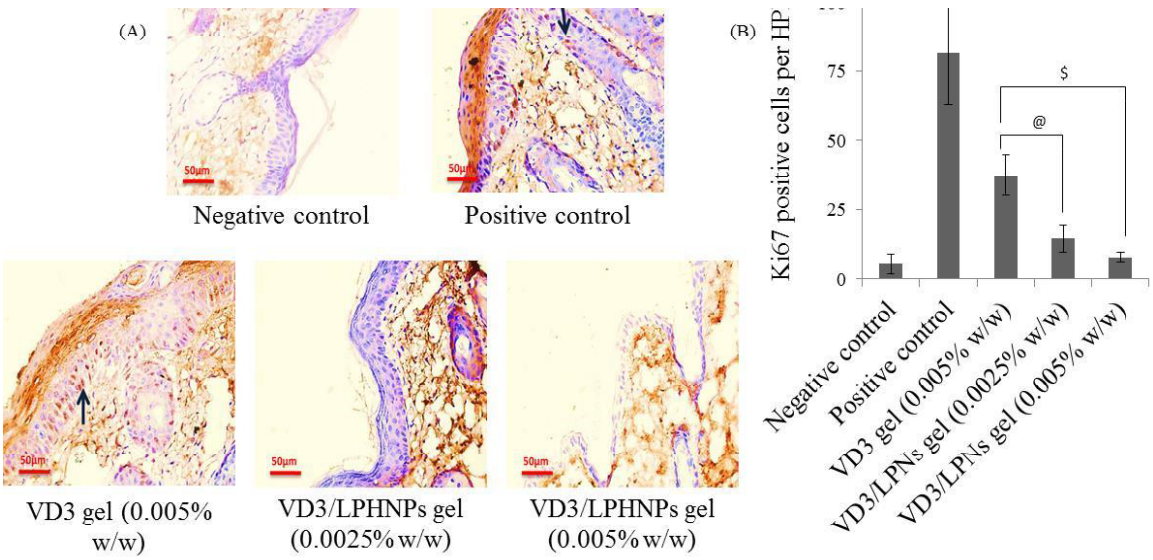

Figure 4.9. (A) Immunohistochemical staining of Ki67, cell proliferation marker expressed in back skin sections of psoriatic mice. Treatment with VD3/LPNs gel efficiently downregulates Ki67 expression (Magnification: 40X, Scale bar = 50 µm). Blue arrow exemplifies the upregulation of Ki67 expression. (B) distribution of average cells positive for Ki67 per High Power Field (HPF) among various groups indicating effectiveness of VD3/LPNs in ameliorating psoriasis. Each value is denoted as mean ± SEM. @, $p \leq 0.05$ and $, $p \leq 0.01$, versus VD3 gel (0.005% w/w) treated group.

pulp as observed in negative control group. Treatment with VD3/LPNs gel (0.005% w/w) resulted into marked improvement in white pulp and a red pulp area of spleen with least sum of total liver and spleen damage score compared to conventional product and was comparable to that of negative control group.

Application of IMQ on the back skin induces severe dermal inflammation followed by hyperplasia of keratinocytes resulting into over-expression of Ki67 (cell proliferation marker). It was observed that animals treated with VD3/LPNs gel showed a significantly lower Ki67 as compared to the free VD3 gel Figure 4.9.

4. Discussion

It is now well recognized that psoriasis is an autoimmune disease of skin resulting into erythema (redness), scaling (peeling) and thickening occurring because of complex interaction between keratinocytes and surrounding dendritic cells [1-3]. The currently accessible therapies for psoriasis can be broadly categorized into systemic, phototherapy, and topical. The systemic therapy and phototherapy are restricted for treating severe type psoriasis due to the associated toxicities [4,5]. Topical therapy approaches are preferred over systemic or phototherapy because of the lower cost and patient compliance. In addition to these advantages, the topical route allows direct targeting of drugs to the stratum basale layer of the epidermis where the pathophysiology of psoriasis originates eliminating unwanted exposure to other organs. Currently, topical nano-drug delivery approaches (including both lipidic and polymeric) are relied as advanced strategies compared to conventional drug delivery systems (ointments, creams and gels) as these facilitated deep skin penetration and imparting slow and sustained drug release profile thus avoiding the

high loco-regional concentration of drug at the applied site eluding unwanted local toxicities and rapid metabolism of drug [19,21-26].

Oral administration of VD3 analogues was not found to be that effective in treating psoriasis with incurring additional hypercalcemic toxic effects [16]. Cholecalciferol (VD3) is synthesized in the skin which is further converted to more potent analogue calcitriol in the presence of enzymes (CYP27A1 and CYP27 B1) within keratinocytes and does not exerts hypercalcemic effect, erythema or burning sensation unlike calcitriol or other analogues [9-15]. The antipsoriatic effects of VD3 and its analogues are well established [11,14,15]. VD3 is a highly lipophilic (log P-7.5) molecule and susceptible to degradation by various modes enforcing challenges for topical delivery. To meet the safety profile of cholecalciferol, a new formulation was prepared that deliver the drug to the deeper skin layers, controls its release profile avoiding rapid metabolism and reduces its systemic absorption and thus avoiding systemic toxicity.

The advantages of lipid-polymer hybrid nanosystem over lipidic and polymeric nano-carrier has been well reported [30]. We have previously reported multi-component clobetasol propionate (CP)-loaded mono-lithic lipid-polymer hybrid nanoparticles that showed significant improvement in the in vivo antipsoriatic efficacy due to deeper skin penetration followed by high cellular uptake, sustained drug release profile with undetectable quantities of drug leaching systemically. We used these LPNs in fabricating VD3/LPNs using mPEG-PLA (amphiphilic copolymer), Precirol® ATO 5 (solid lipid) and linoleic acid (liquid lipid) that previously proved to produce stable nanoparticles over a study period of six months at 2-8°C and RT when formulated into carbopol based hydrogel.

VD3/LPNs thus prepared demonstrated spherical morphology with no significant aggregation observed from FE-SEM images. VD3/LPNs showed slow and sustained drug release profile which was due to the entrapment of drug in central complex hydrophobic core consisting of lipids (liquid and solid), and hydrophobic block of amphiphilic copolymer. These VD3/LPNs were further formulated into Carbopol 974P (0.75% w/w) based topical hydrogel wherein we have used propylene glycol (humectant), methylparaben and propylparaben (preservative) and sodium hydroxide (pH adjusting agent). Successful entrapment of the drug inside the hydrophobic core of LPNs was demonstrated from the FTIR and DSC suggesting its conversion to amorphous state. The rheological studies indicated that VD3/LPNs gel exhibited non-newtonian flow behavior possessing shear-thinning properties which is desirable for slow extrusion of product from the tube upon application of pressure.

In vivo efficacy studies carried out using IMQ-induced psoriasis mouse model revealed that animals treated with VD3/LPNs gel (0.005% w/w) showed significantly improved PASI parameters compared to VD3 gel (0.005% w/w). In addition to this, VD3/LPNs gel (0.005% w/w) treated animals demonstrated a significant reduction in both right ear (ES) and back skin (BS) thickness compared to free VD3 gel. The spleen being the biggest immune system organ is a very sensitive indicator of immune activation or suppression throughout the body of animal. Its increased weight (splenomegaly) may reveal the increased amount of cells in the spleen, reflecting the progression of the disease due to immune stimulation. Splenomegaly associated due to topical application of IMQ is well reported that can be taken into consideration as an important parameter for evaluating antipsoriatic efficacy of any topical formulations [22]. Furthermore, induction of liver fibrosis (hepatic damage) is accompanied by cutaneous inflammation associated due to topical application of IMQ as demonstrated previously in IMQ-

induced psoriasis like mouse model [34]. In this research work data demonstrated that, there was no significant difference in size and an average weight of spleen from VD3/LPNs gel (0.005% w/w) treated group and negative control that indicated the effectiveness of treatment. Even on dose reduction (at half strength i.e. 0.0025% w/w), VD3/LPNs gel was able to significantly improve PASI parameters and average spleen weights compared to the group treated with free VD3 gel with comparable results for the right ear and back skin thickness. Hematoxylin and Eosin stained histopathological samples of right ear skin (ES), back skin (BS), liver and spleen indicated, least overall total tissue damage score for VD3/LPNs gel (0.005% w/w). Even at half dose strength i.e. 0.0025% w/w, VD3/LPNs gel was able to significantly reduce the total damage score for all the above-stated samples compared to VD3 gel (0.005% w/w) indicating an enhancement in the antipsoriatic efficacy of VD3 when delivered as LPH nanoparticle. Keratinocyte hyperplasia associated with psoriasis results in a high expression of Ki67 protein (a cell proliferation marker) whose level of expression is an index of the extent of psoriasis involving direct correlation. The immunohistochemistry (IHC) data revealed a significantly reduced score of an average number of Ki67 positive cells stained per high power field in the group treated with VD3/LPNs gel compared to free VD3 gel. This significant improvement in the efficacy of the LPNs might be accredited to the penetration in deeper viable skin layers, enhanced cellular uptake, and sustained drug release.

5. Conclusion

Current work demonstrated the extended application of our previously established monolithic lipid-polymer hybrid nanoparticles for encapsulating hydrophobic drug molecules. In

this present work, cholecalciferol or VD3 was encapsulated within these multi-component systems comprising of lipids (liquid and solid) and an amphiphilic di-block copolymer (mPEG-PLA). These VD3/LPNs demonstrated spherical morphology and sustained release profile without any burst effect. In vivo antipsoriatic efficacy of VD3 loaded lipid-polymer hybrid nanoparticles in IMQ-induced psoriatic mice model demonstrated improved efficacy of the drug when delivered as LPNs nanosystem. This monolithic LPNs system could serve as a platform for delivering hydrophobic drugs with improved efficacy which was due to higher cellular uptake and deeper skin penetration.

References

[1] T. Dainichi, A. Kitoh, A. Otsuka, S. Nakajima, T. Nomura, D.H. Kaplan, K. Kabashima, The epithelial immune microenvironment (EIME) in atopic dermatitis and psoriasis, Nat Immunol, 19 (2018) 1286-1298.

[2] M.A. Lowes, A.M. Bowcock, J.G. Krueger, Pathogenesis and therapy of psoriasis, Nature, 445 (2007) 866-873.

[3] Y.S. Lee, M.H. Lee, H.J. Kim, H.R. Won, C.H. Kim, Non-thermal atmospheric plasma ameliorates imiquimod-induced psoriasis-like skin inflammation in mice through inhibition of immune responses and up-regulation of PD-L1 expression, Sci Rep, 7 (2017) 15564-017-15725-7.

[4] A.B. Gottlieb, Psoriasis: emerging therapeutic strategies, Nat Rev Drug Discov, 4 (2005) 19-34.

[5] M. Sala, A. Elaissari, H. Fessi, Advances in psoriasis physiopathology and treatments: Up to date of mechanistic insights and perspectives of novel therapies based on innovative skin drug delivery systems (ISDDS), J Control Release, 239 (2016) 182-202.

[6] Murphy. C Emily, Schaffter W Samuel & Friedman J Adam, Nanotechnology for Psoriasis Therapy, Curr Dermatol Rep, 8 (2019) 14-25.

[7] M. Lebwohl, P.T. Ting, J.Y. Koo, Psoriasis treatment: traditional therapy, Ann Rheum Dis, 64 Suppl 2 (2005) ii83-6.

[8] A. Menter, C.E. Griffiths, Current and future management of psoriasis, Lancet, 370 (2007) 272-284.

[9] D.D. Bikle, M.K. Nemanic, E. Gee, P. Elias, 1,25-Dihydroxyvitamin D3 production by human keratinocytes. Kinetics and regulation, J Clin Invest, 78 (1986) 557-566.

[10] D.D. Bikle, M.K. Nemanic, J.O. Whitney, P.W. Elias, Neonatal human foreskin keratinocytes produce 1,25-dihydroxyvitamin D3, Biochemistry, 25 (1986) 1545-1548.

[11] B. Lehmann, The vitamin D3 pathway in human skin and its role for regulation of biological processes, Photochem Photobiol, 81 (2005) 1246-1251.

[12] B. Lehmann, W. Sauter, P. Knuschke, S. Dressler, M. Meurer, Demonstration of UVB-induced synthesis of 1 alpha,25-dihydroxyvitamin D3 (calcitriol) in human skin by microdialysis, Arch Dermatol Res, 295 (2003) 24-28.

[13] D.D. Bikle, Vitamin D and the skin: Physiology and pathophysiology, Rev Endocr Metab Disord, 13 (2012) 3-19.

[14] S. Popadic, Z. Ramic, L. Medenica, M. Mostarica Stojkovic, V. Trajkovic, D. Popadic, Antiproliferative effect of vitamin A and D analogues on adult human keratinocytes in vitro, Skin Pharmacol Physiol, 21 (2008) 227-234.

[15] T.C. Chen, K.S. Persons, Z. Lu, J.S. Mathieu, M.F. Holick, An evaluation of the biologic activity and vitamin D receptor binding affinity of the photoisomers of vitamin D3 and previtamin D3, J Nutr Biochem, 11 (2000) 267-272.

[16] M.A. Ingram, M.B. Jones, W. Stonehouse, P. Jarrett, R. Scragg, O. Mugridge, P.R. von Hurst, Oral vitamin D3 supplementation for chronic plaque psoriasis: a randomized, double-blind, placebo-controlled trial, J Dermatolog Treat, 29 (2018) 648-657.

[17] A. Lalloz, M.A. Bolzinger, J. Faivre, P.L. Latreille, A. Garcia Ac, C. Rakotovao, J.M. Rabanel, P. Hildgen, X. Banquy, S. Briancon, Effect of surface chemistry of polymeric nanoparticles on cutaneous penetration of cholecalciferol, Int J Pharm, 553 (2018) 120-131.

[18] T. Ramezanli, B.E. Kilfoyle, Z. Zhang, B.B. Michniak-Kohn, Polymeric nanospheres for topical delivery of vitamin D3, Int J Pharm., 516 (2017) 196-203.

[19] S.S. Pukale, S. Sharma, M. Dalela, A.K. Singh, S. Mohanty, A. Mittal, D. Chitkara, Multi-component clobetasol-loaded monolithic lipid-polymer hybrid nanoparticles ameliorate imiquimod-induced psoriasis-like skin inflammation in Swiss albino mice, Acta Biomater, 115 (2020) 393-409.

[20] Z. Zhang, P.C. Tsai, T. Ramezanli, B.B. Michniak-Kohn, Polymeric nanoparticles-based topical delivery systems for the treatment of dermatological diseases, Wiley Interdiscip Rev Nanomed Nanobiotechnol, 5 (2013) 205-218.

[21] Pajaree Sakdiset, Thanaporn Amnuaikit, Wiwat Pichayakorn, Sirirat Pinsuwan, Formulation development of ethosomes containing indomethacin for transdermal delivery, J Drug Deliv Sci Technol, 52 (2019) 760-760-768.

[22] L. Sun, Z. Liu, L. Wang, D. Cun, H.H.Y. Tong, R. Yan, X. Chen, R. Wang, Y. Zheng, Enhanced topical penetration, system exposure and anti-psoriasis activity of two particle-sized, curcumin-loaded PLGA nanoparticles in hydrogel, J Control Release, 254 (2017) 44-54.

[23] T. Senyigit, F. Sonvico, S. Barbieri, O. Ozer, P. Santi, P. Colombo, Lecithin/chitosan nanoparticles of clobetasol-17-propionate capable of accumulation in pig skin, J Control Release, 142 (2010) 368-373.

[24] P.P. Shah, P.R. Desai, A.R. Patel, M.S. Singh, Skin permeating nanogel for the cutaneous co-delivery of two anti-inflammatory drugs, Biomaterials, 33 (2012) 1607-1617.

[25] P.R. Desai, S. Marepally, A.R. Patel, C. Voshavar, A. Chaudhuri, M. Singh, Topical delivery of anti-TNFalpha siRNA and capsaicin via novel lipid-polymer hybrid nanoparticles efficiently inhibits skin inflammation in vivo, J Control Release, 170 (2013) 51-63.

[26] P. Desai, R.R. Patlolla, M. Singh, Interaction of nanoparticles and cell-penetrating peptides with skin for transdermal drug delivery, Mol Membr Biol, 27 (2010) 247-259.

[27] A. Kaur, S.S. Katiyar, V. Kushwah, S. Jain, Nanoemulsion loaded gel for topical co-delivery of clobitasol propionate and calcipotriol in psoriasis, Nanomedicine, 13 (2017) 1473-1482.

[28] R. Sonawane, H. Harde, M. Katariya, S. Agrawal, S. Jain, Solid lipid nanoparticles-loaded topical gel containing combination drugs: an approach to offset psoriasis, Expert Opin Drug Deliv, 11 (2014) 1833-1847.

[29] R. Arora, S.S. Katiyar, V. Kushwah, S. Jain, Solid lipid nanoparticles and nanostructured lipid carrier-based nanotherapeutics in treatment of psoriasis: a comparative study, Expert Opin Drug Deliv, 14 (2017) 165-177.

[30] T. Date, V. Nimbalkar, J. Kamat, A. Mittal, R.I. Mahato, D. Chitkara, Lipid-polymer hybrid nanocarriers for delivering cancer therapeutics, J Control Release, 271 (2018) 60-73.

[31] S. Horvath, R. Komlodi, A. Perkecz, E. Pinter, R. Gyulai, A. Kemeny, Methodological refinement of Aldara-induced psoriasiform dermatitis model in mice, Sci Rep, 9 (2019) 3685-019-39903-x.

[32] J.Y. Kim, J. Ahn, J. Kim, M. Choi, H. Jeon, K. Choe, D.Y. Lee, P. Kim, S. Jon, Nanoparticle-Assisted Transcutaneous Delivery of a Signal Transducer and Activator of Transcription 3-Inhibiting Peptide Ameliorates Psoriasis-like Skin Inflammation, ACS Nano, 12 (2018) 6904-6916.

[33] N.W. Kang, M.H. Kim, S.Y. Sohn, K.T. Kim, J.H. Park, S.Y. Lee, J.Y. Lee, D.D. Kim, Curcumin-loaded lipid-hybridized cellulose nanofiber film ameliorates imiquimod-induced psoriasis-like dermatitis in mice, Biomaterials, 182 (2018) 245-258.

[34] P. Vasseur, M. Pohin, J.F. Jegou, L. Favot, N. Venisse, J. Mcheik, F. Morel, J.C. Lecron, C. Silvain, Liver fibrosis is associated with cutaneous inflammation in the imiquimod-induced murine model of psoriasiform dermatitis, Br J Dermatol, 179 (2018) 101-109.